

# Aligned Carbon Nanotube Sheets for the Electrodes of Organic Solar Cells

Zhibin Yang, Tao Chen, Ruixuan He, Guozhen Guan, Houpu Li, Longbin Qiu, and Huisheng Peng\*

Platinum or/and indium tin oxide have been used for electrodes in the fabrication of various optoelectronic and electronic devices.<sup>[1–6]</sup> However, there remain a few critical disadvantages that have greatly limited their future applications. For instance, there are limited sources for both platinum and indium on the earth, a high temperature or a vacuum process is generally required to prepare them on substrates with high costs, and they are also unstable during applications (e.g., platinum may be dissolved in corrosive electrolytes and indium tin oxide is not resistant to an acid).<sup>[4–6]</sup> Therefore, new electrode materials with good stability, high efficiency, and low cost are highly desired. Recently, increasing attention has been paid to carbon nanotubes (CNTs), which may represent promising electrode materials to simultaneously solve the above challenges due to their unique structures and excellent mechanical and electrical properties.<sup>[7–17]</sup> For instance, CNTs were used to replace the platinum in counter electrodes to catalyze the reduction of triiodide in dye-sensitized solar cells with the target of better performances.<sup>[7–9]</sup> However, the improvements have been far from what was expected due to the random dispersion of CNTs, which largely decreases their capabilities for charge separation and transport. Herein, we have developed aligned CNT sheets with good transparency, high flexibility, and excellent electronic properties as a family of new electrode materials. A dye-sensitized solar cell created by using the CNT sheet in the counter electrode, as an application example, has been demonstrated to have significantly improved performance. The energy conversion efficiency of the resulting cell is higher than the randomly dispersed CNT film and comparable with the platinum. Particularly, novel and flexible solar cells can be easily made from the CNT sheet with great potentials.

To prepare the CNT sheets, CNT arrays were first synthesized with Fe/Al<sub>2</sub>O<sub>3</sub> as the catalyst, ethylene as the carbon source, and an Ar/H<sub>2</sub> mixture as the carrying gas during a chemical vapor deposition process. A CNT array with a thickness of ≈300 μm was used in this work unless otherwise specified. The CNT sheets with lengths of meters could then be directly spun from the array on a large scale. **Figure 1a** shows a scanning electron

microscopy (SEM) image of a typical CNT sheet with a uniform width and thickness. The sheet width may be controlled in the range of millimeters to centimeters by varying the initial ribbon width during the spinning process, and the thicknesses are typically tens of nanometers. Here we mainly study multiwalled CNTs with an average diameter of ≈7 nm (**Figure 1b**) due to their easy synthesis. The CNTs are highly aligned along the sheet (**Figure S1**, Supporting Information), and their average number density is calculated to be ≈10<sup>11</sup> cm<sup>-2</sup> with a weight density of ≈8.4 mg cm<sup>-3</sup>.

The CNT sheets are transparent from 20 to 100 nm in thickness. **Figure 1c** shows a typical optical image of the CNT sheet with a thickness of 20 nm on a marked paper. The underlying words can be clearly observed. UV-vis spectroscopy further indicates high transmittance from 300 to 800 nm (**Figure S2**, Supporting Information). As expected, these CNT sheets show high flexibility (**Figure 1d**), and they can be bent for many cycles without observable structure changes traced by SEM. Due to the highly aligned organization of the CNTs, the resulting sheets show remarkable electronic properties. The electrical conductivity along the CNT sheet was measured on the level of 10<sup>2</sup>–10<sup>3</sup> S cm<sup>-1</sup> at room temperature. To investigate their application potentials as electrodes, and particularly as flexible electrodes, electrical conductivities of the CNT sheets were further examined under bending. **Figure 1e,f** compare the electrical conductivities of a CNT sheet stabilized on poly(ethylene terephthalate) after being bent one hundred times in the direction parallel and vertical to the aligned CNTs, respectively. Obviously, the conductivities remained almost unchanged during the deformable processes in both cases.

As an application example, the CNT sheets were used in counter electrodes to replace platinum in the fabrication of dye-sensitized solar cells. **Figure 2** schematically shows a typical cell structure. The detailed fabrications are discussed in the Experimental Section. To summarize, the working electrode (composed of TiO<sub>2</sub> nanoparticles and a N719 dye) and the counter electrode (using a CNT sheet) were first sealed with a Surlyn frame as the spacer between them. The redox electrolyte, which consisted of LiI, I<sub>2</sub>, 1,2-dimethyl-3-propylimidazolium iodide, GuSCN, and tri-butyl-phosphate in the dehydrated acetonitrile, was then injected into the cell. The working mechanism may be briefly described as follows: dye molecules are excited by absorbing photons and inject electrons into the conduction band of TiO<sub>2</sub>. Electrons move along the external circuit and arrive at the CNT sheet, where I<sup>3-</sup> ions are reduced to I<sup>-</sup> ions. Dye molecules are finally regenerated by the I<sup>-</sup> ions to complete a cycle. CNTs had been widely studied to catalyze the reduction reaction of I<sup>3-</sup> ions, and the aligned CNT sheet with a high

Z. Yang, T. Chen, R. He, G. Guan, H. Li, L. Qiu, Prof. H. Peng  
Key Laboratory of Molecular Engineering of Polymers of  
Ministry of Education  
Department of Macromolecular Science  
and Laboratory of Advanced Materials  
Fudan University  
Shanghai 200438, China  
E-mail: penghs@fudan.edu.cn

DOI: 10.1002/adma.201103509

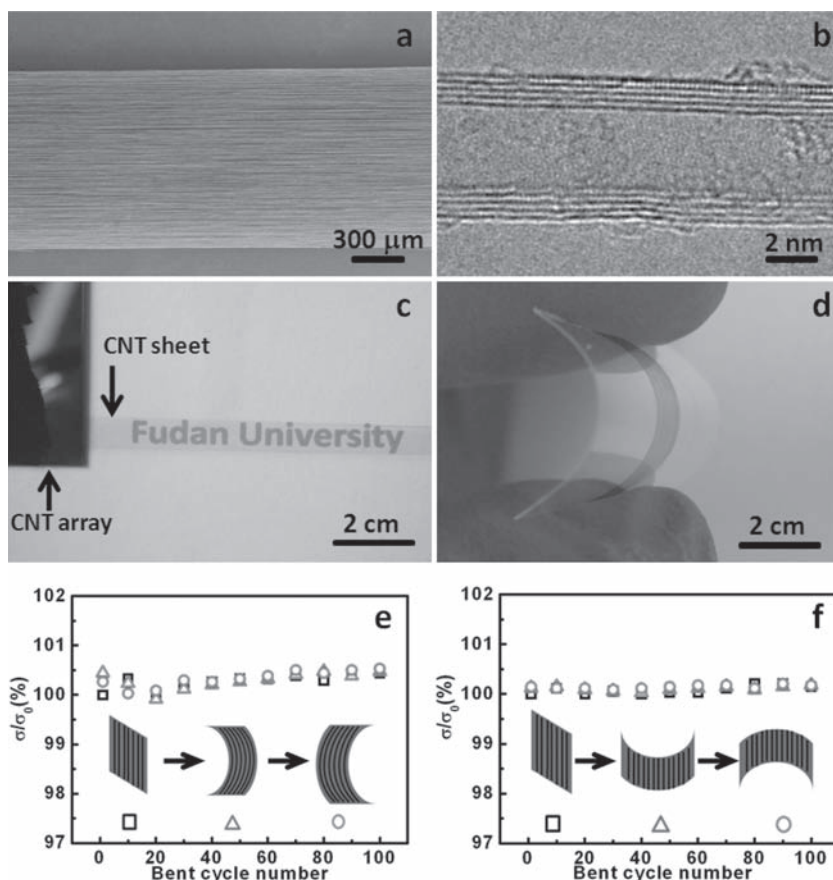


**Figure 1.** Structures and electrical properties of the CNT sheet. a) SEM image of a CNT sheet. b) High-resolution transmission electron microscopy (TEM) image of a CNT. c) Optical image of a CNT sheet with thickness of 20 nm on a marked paper. d) A flexible CNT sheet on the poly(ethylene terephthalate) film. e) Electrical conductivities of a CNT sheet under bending along the CNT-aligned direction.  $\sigma_0$  and  $\sigma$  correspond to the electrical conductivities of the CNT sheet before and after bending. f) Electrical conductivities of a CNT sheet under bending vertical to the CNT-aligned direction.

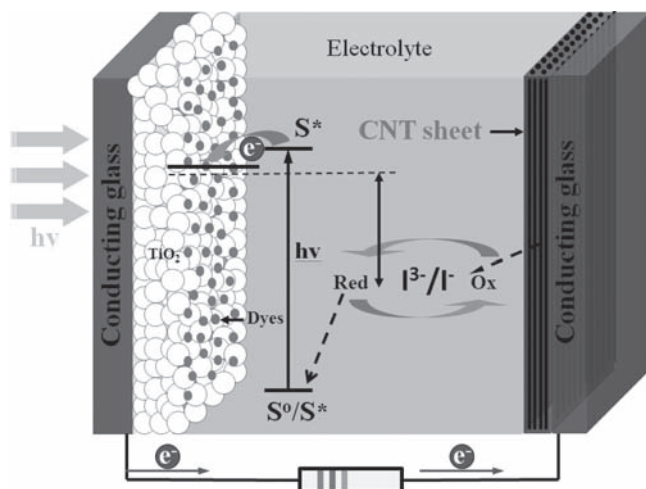


**Figure 2.** Schematic illustration of a novel dye-sensitized solar cell using a CNT sheet as the counter electrode.

electrical conductivity further improves the catalysis, so the resulting cells are expected to show high performance.

Dye-sensitized solar cells with the aligned CNT sheet, the randomly dispersed pristine CNT film, and the platinum as counter electrodes were first investigated and compared under the same experimental conditions in **Figure 3**. For the CNT sheet, the resulting dye-sensitized solar cell typically exhibited an open-circuit photovoltage ( $V_{OC}$ ) of 0.67 V, short-circuit photocurrent density ( $J_{SC}$ ) of  $10.80 \text{ mA cm}^{-2}$ , and fill factor ( $FF$ ) of 0.57. The energy conversion efficiency ( $\eta$ ) is calculated to be 4.18%. As a comparison, the cell derived from the randomly dispersed pristine CNT film typically showed a  $V_{OC}$  of 0.67 V,  $J_{SC}$  of  $8.11 \text{ mA cm}^{-2}$ , and  $FF$  of 0.59 with  $\eta$  of 3.24%. Currently, the cell efficiencies based on the CNT sheet and the randomly disperses CNT film are mainly (3.78–4.24)% and (3.02–3.31)%, respectively. Therefore, the energy conversion efficiency has been greatly increased after the alignment of CNTs. Compared with the platinum, the cell derived from the CNT sheet without optimizations showed the same  $V_{OC}$  but slightly decreased  $J_{SC}$  and  $FF$ .

To further investigate the application potential of the CNT sheet in counter electrodes in dye-sensitized solar cells, electrochemical impedance spectroscopy was used to compare the cells derived from the CNT sheet and the platinum. For a dye-sensitized solar cell, the series resistance includes three parts with three semicircles in an impedance

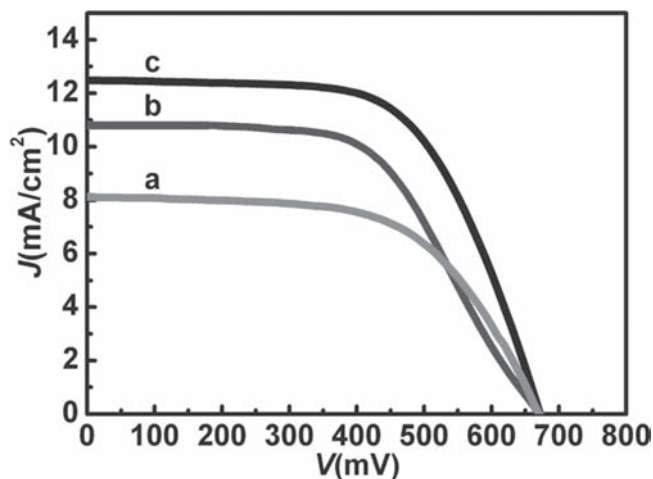


**Figure 3.** Current–voltage characteristics of the typical dye-sensitized solar cells by using the randomly dispersed pristine CNT film (a), the aligned multiwalled CNT sheet (b), and the platinum (c) as counter electrodes. The curves were obtained under AM 1.5 illumination.

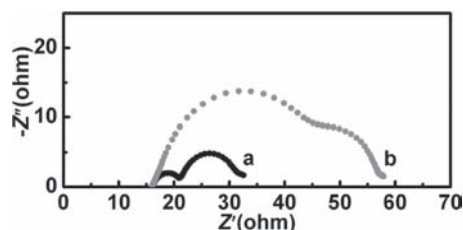


**Figure 4.** Nyquist plots of dye-sensitized solar cells by using the platinum (a) and the CNT sheet (b) as counter electrodes measured under AM 1.5 illumination. The frequencies were ranged from 0.1 to 100 kHz with an applied voltage of  $-0.8$  V.

spectrum. The first semicircle reflects the electrochemical reaction at the counter electrode in the high-frequency region, the second semicircle represents the charge transfer at  $\text{TiO}_2/\text{dye}/\text{electrode}$  interfaces in the middle-frequency region, and the third semicircle shows the Warburg diffusion process of  $\text{I}^-$  and  $\text{I}_3^-$  ions in the electrolyte in the low-frequency region. Therefore, the catalytic properties of the CNT sheet can be directly estimated from the first semicircle. As shown in **Figure 4**, the first semicircle of the cell based on the CNT sheet is larger than that derived from the platinum. The larger first semicircle increases the series resistance, which may reduce the FF of the cell. In other words, the cell efficiency based on a CNT sheet can be further greatly improved by a decrease in the resistance (or an increase in the conductivity), which had been realized by the increase in the length of used CNTs. For instance, the CNT sheet was improved by more than two times in the conductivity when the CNTs were lengthened by about two times.

We have further investigated dye-sensitized solar cells by using a series of CNT sheets with different numbers of layers (1, 3, 5, 7, and 9) as the counter electrodes under the same experimental conditions. As the thickness of one layer of CNT sheet is  $\approx 20$  nm, the above CNT sheets show increasing thicknesses of  $\approx 20, 60, 100, 140,$  and  $180$  nm, respectively. The main parameters of  $V_{\text{OC}}, J_{\text{SC}}, FF,$  and  $\eta$  of the resulting cells have been compared in **Figure 5**. The values of  $V_{\text{OC}}, J_{\text{SC}},$  and  $FF$  remain almost unchanged with the increase in the sheet thickness.

Due to the high flexibility, CNT sheets were also used as counter electrodes to fabricate flexible dye-sensitized solar cells (**Figure S4**, Supporting Information). A representative  $J-V$  curve of a flexible cell using three layers of CNT sheets as the counter electrode is shown in **Figure S5** (Supporting Information). The values of  $V_{\text{OC}}, J_{\text{SC}},$  and  $FF$  are  $0.68$  V,  $4.84$   $\text{mA cm}^{-2}$ , and  $0.37$ , respectively. The energy conversion efficiency of the flexible cell can be increased to be close to a rigid cell by improving the fabrication process.

It should be emphasized that the above dye-sensitized solar cells based on the CNT sheet have not been optimized with respect to the material used, the structure of the CNT

sheet, or the device architecture. The efficiency of the resulting cell can be greatly enhanced after the optimization of the experimental parameters. For instance, for the CNT sheet with an increased conductivity spun from a CNT array with the higher thickness of  $1.20$  mm, the resulting cell showed an efficiency of  $6.60\%$  compared with  $5.27\%$  of the platinum-based cell under the same conditions. More efforts are also underway to further improve the conductivity of the CNT sheet by the enhancement in the CNT quality (fewer impurities and defects) and the increase in the CNT number density.

In summary, we have explored the aligned CNT sheet as the counter electrode to fabricate dye-sensitized solar cells with efficiencies higher than the randomly dispersed CNT film and comparable with platinum. In addition to the application in the replacement of the platinum, the CNT sheets are also a promising candidate to replace indium tin oxide in various optoelectronic and electronic devices, particularly in flexible devices, due to their excellent mechanical and electrical properties.

## Experimental Section

CNT arrays were first synthesized by a chemical vapor deposition in a quartz tube furnace by using  $\text{Fe}$  ( $1$  nm)/ $\text{Al}_2\text{O}_3$  ( $10$  nm) on a silicon wafer as the catalyst, ethylene as carbon source, and a mixture of Ar and  $\text{H}_2$  gases as the carrying gas, typically at  $750$   $^\circ\text{C}$ .<sup>[18,19]</sup> The CNT sheet was spun from a CNT array by using a blade. The blade was touched to adhere to the edge part of a spinnable CNT array and then continuously pulled out to form a CNT sheet. Finally, the CNT sheet was transferred onto FTO ( $\text{F-doped SnO}_2$ ,  $15$   $\text{ohm square}^{-1}$ , transmittance  $90\%$ , Nippon Sheet Glass Co., Japan) or flexible ITO (indium tin oxide) on PEN substrates ( $15$   $\text{ohm square}^{-1}$ , Peccell Co., Japan). The CNT sheets were stabilized on the substrates after the solvent treatment using ethanol

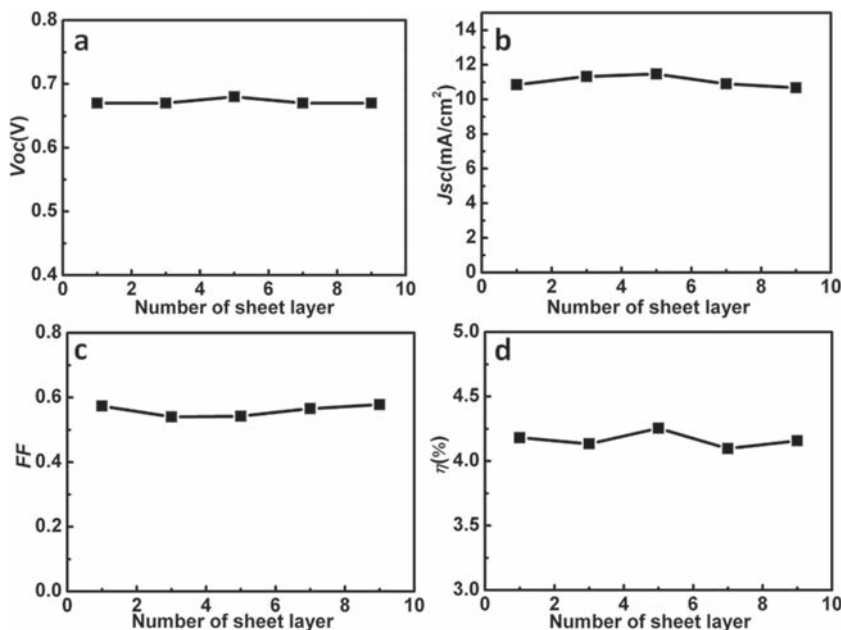


**Figure 5.** Dependence of the dye-sensitized solar cell on the layer number of the CNT sheet. a) Dependence of the open-circuit photovoltage on the layer number. b) Dependence of the short-circuit photocurrent density on the layer number. c) Dependence of the fill factor on the layer number. d) Dependence of the efficiency on the layer number.

and the annealing treatment was 500 °C in argon in the case of FTO or 150 °C in air in the case of ITO-PEN. The randomly dispersed pristine CNT film was prepared by coating a pure pristine CNT dispersion in cyclohexyl-pyrrolidone (concentration of 3 mg mL<sup>-1</sup>) onto FTO.

A nanocrystalline TiO<sub>2</sub> layer (thickness of 10 μm) was coated onto FTO to prepare a working electrode through a printing technology. In order to optimize the TiO<sub>2</sub> morphologies to improve the dye absorption, the working electrode was heated to 120 °C and then immersed into a N719 dye solution in acetonitrile/tert-butanol (volume ratio of 1/1, concentration of 0.5 mM) for 16 h. The N719-incorporated working electrode was rinsed with acetonitrile. The working and counter electrodes with a Surllyn frame as the spacer were sealed by pressing them together at a pressure of ≈0.2 MPa and a temperature of 125 °C. The redox electrolyte which consists of LiI, I<sub>2</sub>, 1,2-dimethyl-3-propylimidazolium iodide, GuSCN, and tri-butyl-phosphate in dehydrated acetonitrile was obtained from Dalian Heptachroma Solartech Co., Ltd. The redox electrolyte was injected into the cell through the back holes of the counter electrode. Finally, the back holes were sealed with the Surllyn and a microscopy cover glass. For the fabrication of a flexible cell, a "P25" powder (obtained from Dalian Heptachroma Solartech Co., Ltd.) with 70% anatase and 30% rutile TiO<sub>2</sub> was added to ethanol with a concentration of 20 wt%. The suspension was coated onto the conducting substrate to produce the working electrode.

## Supporting Information

Supporting Information is available from the Wiley Online Library or from the author.

## Acknowledgements

The authors thank Dr. Q. Shen at SIMIT for the catalyst support and Dr. Z. Wang for the useful discussion. This work was supported by NNSFC (20904006, 91027025), MOST (2011CB932503, 2011DFA51330), MOE (NCET-09-0318), STCSM (1052nm01600, 09PJ1401100), Li Foundation Heritage Prize, and Fudan University.

Received: September 12, 2011

Published online: October 24, 2011

- [1] Q. Zhang, G. Cao, *Nano Today* **2011**, *6*, 91.
- [2] A. Hagfeldt, G. Boschloo, L. Sun, L. Kloo, H. Pettersson, *Chem. Rev.* **2010**, *110*, 6595.
- [3] E. Ramasamy, W. J. Lee, D. Y. Lee, J. S. Song, *Electrochem. Commun.* **2008**, *10*, 1087.
- [4] W. J. Lee, E. Ramasamy, D. Y. Lee, J. S. Song, *ACS Appl. Mater. Interfaces* **2009**, *1*, 1145.
- [5] Y. Huang, E. M. Terentjev, *ACS Nano* **2011**, *5*, 2082.
- [6] J. A. Rogers, T. Someya, Y. G. Huang, *Science* **2010**, *327*, 1603.
- [7] J. E. Trancik, S. C. Barton, J. Jone, *Nano Lett.* **2008**, *8*, 982.
- [8] H. Zhu, H. Zeng, V. Subramanian, C. Masarapu, K. Huang, B. Wei, *Nanotechnology* **2008**, *19*, 465204.
- [9] W. J. Lee, E. Ramasamy, D. Y. Lee, J. S. Song, *ACS Appl. Mater. Interfaces* **2009**, *1*, 1145.
- [10] M. Gratzel, *Acc. Chem. Res.* **2009**, *42*, 1788.
- [11] C. Yen, Y. Lin, S. Liao, C. Weng, C. Huang, Y. Hsiao, C. M. Ma, M. Chang, H. Shao, M. Tsai, C. Hsieh, C. Tsai, F. Weng, *Nanotechnology* **2008**, *19*, 375305.
- [12] E. Ramasamy, W. J. Lee, D. Y. Lee, J. S. Song, *Electrochem. Commun.* **2008**, *10*, 1087.
- [13] T. Chen, S. Wang, Z. Yang, Q. Feng, X. Sun, L. Li, Z. Wang, H. Peng, *Angew. Chem. Int. Ed.* **2011**, *50*, 1815.
- [14] G. Li, F. Wang, Q. Jiang, X. Gao, P. Shen, *Angew. Chem. Int. Ed.* **2010**, *49*, 3653.
- [15] K. Huang, Y. Wang, R. Dong, W. Tsai, K. Tsai, C. Wang, Y. Chen, R. Vittal, J. Lin, K. Ho, *J. Mater. Chem.* **2010**, *20*, 4067.
- [16] R. Ulbricht, S. B. Lee, X. Jiang, K. Inoue, M. Zhang, S. Fang, R. H. Raughman, A. A. Zakhidov, *Sol. Energy Mater. Sol. Cells* **2007**, *91*, 416.
- [17] T. Chen, Z. Cai, Z. Yang, L. Li, X. Sun, T. Huang, A. Yu, H. G. Kia, H. Peng, *Adv. Mater.* **2011**, *23*, 10.1002/adma.201102200.
- [18] L. Zheng, G. Sun, Z. Zhan, *Small* **2010**, *6*, 132.
- [19] a) L. Li, Z. Yang, H. Gao, H. Zhang, J. Ren, X. Sun, T. Chen, H. G. Kia, H. Peng, *Adv. Mater.* **2011**, *23*, 3730; b) S. Huang, L. Li, Z. Yang, L. Zhang, H. Saiyin, T. Chen, H. Peng, *Adv. Mater.* **2011**, *23*, 10.1002/adma.201102472; c) H. Peng, X. Sun, F. Cai, X. Chen, Y. Zhu, G. Liao, D. Chen, Q. Li, Y. Lu, Y. Zhu, Q. Jia, *Nat. Nanotechnol.* **2009**, *4*, 738; d) H. Peng, X. Sun, *Chem. Commun.* **2009**, 1058; e) H. Peng, X. Sun, *Chem. Phys. Lett.* **2009**, *471*, 103.